Overview of the QPS Project

J.F. Lyon[1], S.P. Hirshman[1], D.A. Spong[1], D.J. Strickler[1], B.E. Nelson[1], A.S. Ware[2], D.E. Williamson[1], L.A. Berry[1], M.J. Cole[1], P.J. Fogarty[1], P.K. Mioduszewski[1], D.A. Monticello[3], G.Y. Fu[3], D. Mikkelsen[3], E. Barcikowski[2], D. Westerly[2]

[1]*Oak Ridge National Laboratory, P.O. Box 2009, Oak Ridge, TN 37831-8072, U.S.A.*
[2]*Department of Physics and Astronomy, University of Montana, Missoula, MT, 59812, U.S.A*
[3]*Princeton Plasma Physics Laboratory, P.O. Box 451, Princeton, NJ 08502, U.S.A*

Abstract. QPS is a very-low-aspect-ratio quasi-poloidally-symmetric stellarator with $\langle R \rangle$ = 0.95–1 m, $\langle a \rangle$ = 0.3–0.4 m, $\langle B_{axis} \rangle$ = 1 T for a 1.5-s pulse, and $P_{heating}$ = 2–4 MW. This paper describes the physics properties and the engineering design of the QPS experiment.

I. MAGNETIC CONFIGURATION AND FLEXIBILITY

A quasi-poloidal stellarator with very low plasma aspect ratio ($\langle R \rangle / \langle a \rangle \sim 2.7$, 1/2-1/4 that of existing stellarators) is a new stellarator magnetic configuration that could ultimately lead to a high-beta, disruption-free, compact stellarator reactor. The Quasi-Poloidal Stellarator (QPS) [1] is being developed to test key features of this approach: robustness of the MHD equilibrium, reduced neoclassical and anomalous transport, and stability limits at $\langle \beta \rangle$ up to 2.5%. The shape of the QPS flux surfaces shown in Fig. 1 varies from bean-shaped at the high-field ends to D-shaped in the middle of the long sections. There is also a large helical excursion of the magnetic axis. The dominant components in the magnetic field expansion

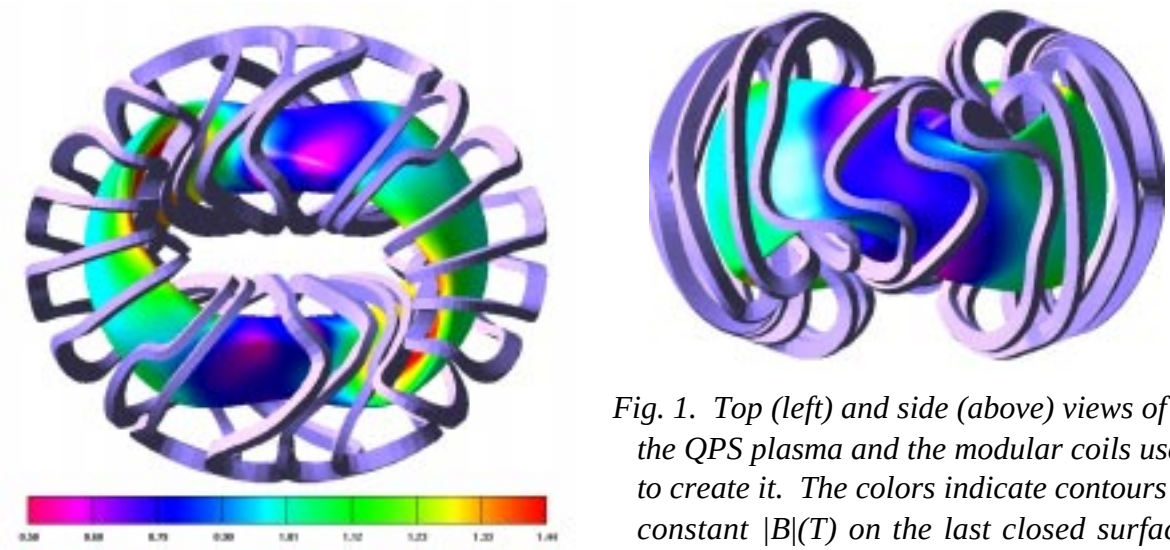

Fig. 1. Top (left) and side (above) views of the QPS plasma and the modular coils used to create it. The colors indicate contours of constant |B|(T) on the last closed surface.

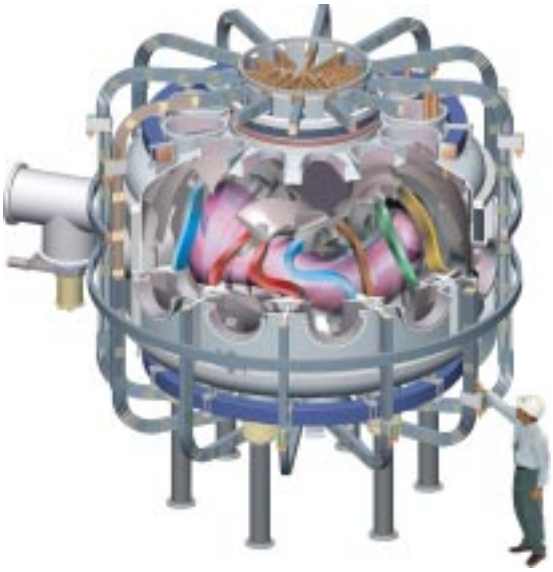

Table 1. QPS Device Parameters

Ave. major radius <*R*>	0.9-1 m
Ave. plasma radius <*a*>	0.3-4 m
Plasma aspect ratio	2.7
Plasma volume V_{plasma}	2-3 m^3
Central, edge rotational transform i_0, i_a	0.21, 0.32
Average field on axis from modular coils	$B_{modular}$ = 1 T for 1.5 s
Auxiliary toroidal field	± 0.15 T
Ohmic current I_{plasma}	≤ 50 kA
ECH power	1.9 MW
ICRF heating power	1.5-3.5 MW

Fig. 2. Cutaway view of QPS.

are poloidally symmetric in "Boozer" flux coordinates, which leads to reduced neoclassical transport and decreased poloidal viscosity. The resulting sheared ambipolar radial electric field provides a source for $\boldsymbol{E} \times \boldsymbol{B}$ poloidal flows and reduction of anomalous transport.

Figure 2 shows the experimental embodiment of the QPS configuration; the main device parameters are listed in Table 1. First plasma operation is planned for 2007. The main coil set has two field periods with 10 modular coils per period. Due to stellarator symmetry, there are only five different coil types. In addition there are three sets of poloidal field coils, toroidal field (TF) coils, and an Ohmic current solenoid. The central bore contains the central legs of the TF coils and the solenoid windings. These coil sets allow plasma shape and position control and driving up to 50 kA of plasma current. Nine independent controls on the coil currents permit a wide range of magnetic configurations.

Figure 3 shows examples of the configuration flexibility. For no electric field in the low-collisionality limit, the neoclassical ripple-induced heat diffusivity is proportional to $\varepsilon_{eff}^{3/2}$ where ε_{eff} is the effective ripple in a single helicity $1/\nu$ transport model that gives the same transport as a full 3-D calculation in this limit. QPS has similar transport to that in the W 7-X configuration, but at 1/4 the plasma aspect ratio. Changes in coil currents allow a factor ~25 variation in the ripple-induced neoclassical heat diffusivity, as shown in Fig. 3(a).

Figure 3(b) shows that changes in the coil currents can produce a factor ~10 variation in the degree of poloidal symmetry as calculated by the ratio U/S of the magnetic energy in the non-symmetric modes (i.e., those with poloidal mode number $m \neq 0$) to those that have poloidal symmetry (with $m = 0$). The fraction of the magnetic energy in non-poloidally

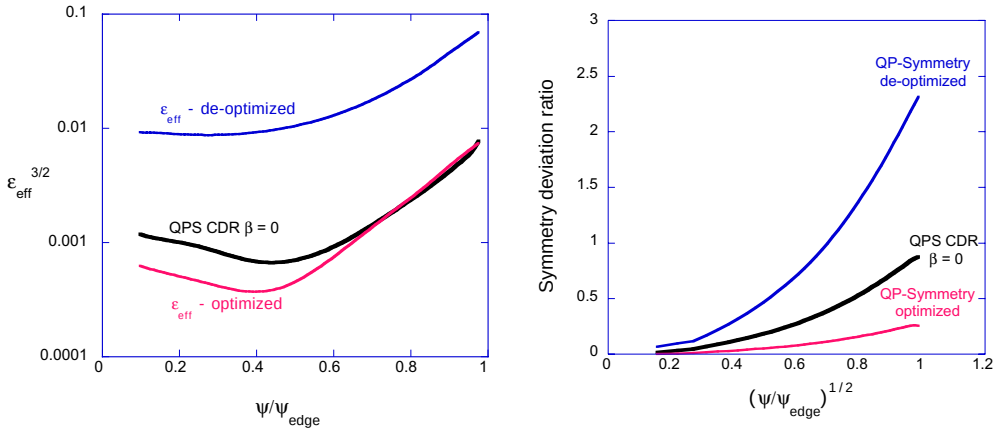

Fig. 3. Changes in the QPS coil currents permit varying (a) neoclassical transport and (b) quasi-poloidal symmetry over a wide range.

symmetric field components is <10% in the plasma core (r/a < 0.4) and rises to ~40% at the plasma edge for the base $\langle\beta\rangle$ = 2% case. Here S excludes the flux surface average magnetic field (m = 0, n = 0) component. Including this term reduces the magnitude of the U/S ratio for the base (CDR) QPS configuration to 0.4% at r/a = 0.4 and 3% at the plasma edge.

Changes in the coil currents also allow a factor of 5–30 variation in the poloidal viscosity, which determines the radial electric field and poloidal rotation, and variation of the rotational transform profile ι(r). Changing only the currents in the toroidal field coils keeps $\iota(0)$ constant and varies $\iota(a)$ from 0.2 to 0.3 with no plasma current. Allowing all coil currents to change keeps $\iota(a)$ constant and varies $\iota(0)$ from 0.1 to 0.25.

II. PERFORMANCE

Figure 4(a) shows the rotational transform (ι) profile and flux surfaces in the D-shaped cross section at $\langle\beta\rangle$ = 2% where an Ohmic current has been added to the bootstrap current to tailor

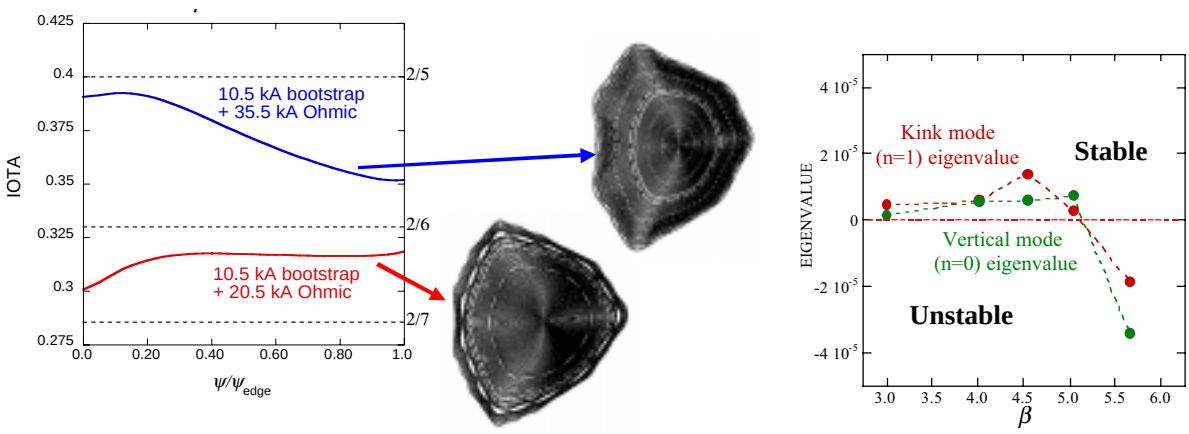

Figure 4. (a) Rotational transform profiles and flux surfaces in the D-shaped cross section at $\langle\beta\rangle$ = 2%; (b) eigenvalues for n = 0 and n = 1 modes.

the ι(r) profile to avoid low-order resonant values of ι. Good flux surfaces are also obtained at $\langle\beta\rangle$ = 3% and 4% using the same approach. The nominal infinite-n ballooning stability limit is 2.5% for the base configuration; the limit rises to 3% with finite-n corrections. However, the validity of these β limits has been called into question by experimental results from LHD and W 7-AS. Figure 4(b) indicates that external kink (n = 1) and vertical (n = 0) modes are stable to $\langle\beta\rangle \approx 5\%$.

1-D transport calculations with self-consistent ambipolar electric fields indicate that $\langle\beta\rangle$ = 2–4% can be obtained if the anomalous heat diffusivity χ_{anom} can be reduced to ~3 m^2/s with large electric field shear as a result of the low poloidal viscosity in QPS. Figure 5 shows the χ_{anom} value needed to give a *combined* confinement time corresponding to a particular ISS-95 confinement [2] multiplier (H-ISS95) for the base QPS configuration and the resulting $\langle\beta\rangle$. Here $\langle n_e\rangle = 10^{20}$ m^{-3}, $P_{heating}$ = 4 MW, and $\langle B\rangle$ = 1 T. The calculated performance depends on the degree of anomalous transport and not on the form for $\chi_{anom}(r)$. The solid red curve uses a constant χ_{anom} and the dashed curve a parabolic χ_{anom} that varies a factor of 10 from the center to the edge; both have the same value at r/a= 0.65. A value for $\chi_{anom} \approx 3$ m^2/s gives H-ISS95 ≈ 2.6 and $\langle\beta\rangle \approx 4.5\%$. The corresponding values for a low-density (2 x 10^{19} m^{-3}) lower-power ($P_{heating}$ = 1.5 MW) case are H-ISS95 ≈ 2.7 and $\langle\beta\rangle \approx 1.4\%$. For this case the central electron temperature drops from 2.7 keV to 1.6 keV for the "ε_{eff} de-optimized" configuration in Fig. 3(a), indicating that neoclassical and anomalous transport can be distinguished in QPS.

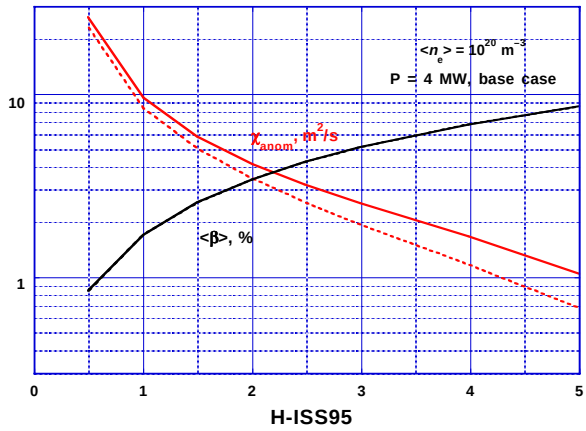

Figure 5. Variation of $\langle\beta\rangle$ and χ_{anom} with the ISS-95 multiplier for the base configuration.

Acknowledgments: This work was supported by the U.S. Dept. of Energy under contract DE-AC05-00OR22725 with UT-Battelle, LLC.

[1] J. F. Lyon and the QPS team, "QPS, A Low Aspect Ratio Quasi-Poloidal Concept Exploration Experiment", http://qps.fed.ornl.gov/.

[2] U. Stroth et al., *Nucl. Fusion* **36**, 1063 (1996).